Toxicology Letters 282 (2018) 71–80

Contents lists available at ScienceDirect

Toxicology Letters

journal homepage: www.elsevier.com/locate/toxlet

Full Length Article

Structure determination of disease associated peak AAA from L-Tryptophan implicated in the eosinophilia-myalgia syndrome

Klaus Klarskov[a], Hugo Gagnon[b], Pierre-Luc Boudreault[a], Chad Normandin[a], Baptiste Plancq[a], Eric Marsault[a], Gerald J. Gleich[c], Stephen Naylor[d,*]

[a] Department of Pharmacology and Physiology, Faculty of Medicine and Health Sciences, Université de Sherbrooke, Sherbrooke, Québec J1H 5N4, Canada
[b] PhenoSwitch Bioscience, Sherbrooke, Quebec J1H 5N4, Canada
[c] Departments of Dermatology and Medicine, School of Medicine, University of Utah, Salt Lake City, UT 84132, USA
[d] ReNeuroGen LLC, Milwaukee, WI 53122, USA

ARTICLE INFO

Keywords:
Eosinophilia myalgia syndrome
Peak AAA
Case-associated
Dietary supplements
Contaminants

ABSTRACT

The eosinophilia-myalgia syndrome (EMS) outbreak of 1989 that occurred in the USA and elsewhere was caused by the ingestion of L-Tryptophan (L-Trp) solely manufactured by the Japanese company Showa Denko K.K. (SD). Six compounds present in the SD L-Trp were reported to be case-associated contaminants. However, "one" of these compounds, Peak AAA has remained structurally uncharacterized, despite the fact that it was described as "the only statistically significant ($p = 0.0014$) contaminant". Here, we employ on-line microcapillary-high performance liquid chromatography-electrospray ionization mass spectrometry (LC–MS), and tandem mass spectrometry (MS/MS) to determine that Peak AAA is in fact two structurally related isomers. Peak AAA_1 and Peak AAA_2 differed in LC retention times, and were determined by accurate mass-LC–MS to both have a protonated molecular ion (MH^{+}) of mass 343.239 Da (Da), corresponding to a molecular formula of $C_{21}H_{30}N_2O_2$, and possessing eight degrees of unsaturation (DoU) for the non-protonated molecule. By comparing the LC–MS and LC–MS-MS retention times and spectra with authentic synthetic standards, Peak AAA_1 was identified as the intermolecular condensation product of L-Trp with anteiso 7-methylnonanoic acid, to afford (*S*)-2-amino-3-(2-((S,E)-7-methylnon-1-en-1-yl)-1H-indol-3-yl)propanoic acid. Peak AAA_2 was determined to be a condensation product of L-Trp with decanoic acid, which produced (*S*)-2-amino-3-(2-((*E*)-dec-1-en-1-yl)-1H-indol-3-yl)propanoic acid.

1. Introduction

The eosinophilia-myalgia syndrome (EMS) is a chronic, multi-systemic disorder characterized by peripheral eosinophilia and sub-acute onset myalgia (Hertzman et al., 2001; Martin et al., 1990). The disease was first identified during October 1989 in three USA patients who were all taking a L-Tryptophan (L-Trp) dietary supplement (Hertzman et al., 1990). Initial epidemiological studies as well as a national surveillance program initiated by the USA based Centers for Disease Control and Prevention (CDC) revealed a strong association between onset of EMS and consumption of L-Trp (Belongia et al., 1990; Belongia 2004; Kilbourne 1992; Swygert et al., 1990; Varga et al., 1993). The USA Food and Drug Administration (FDA) promptly responded, and on November 11th, 1989 issued a nationwide alert advising consumers to stop consumption of manufactured L-Trp food products. They also requested a nationwide recall of all L-Trp supplements sold over-the-counter. The ensuing aftermath resulted in over 1500 patients being afflicted with EMS, and at least 36 deaths were directly attributed to consumption of L-Trp in the USA alone (Swygert et al., 1993). Numerous additional EMS cases were reported worldwide including the UK, Germany, Canada, Belgium, France, Israel and Japan (Hertzman et al., 1991; UK Committee on Toxicology, 2004). Subsequent analyses by individual USA State health departments and the CDC indicated that EMS was triggered by the consumption of L-Trp manufactured by a single company, Showa Denko K.K. (SD) of Japan (Eidson et al., 1990; Philen et al., 1993; Slutsker et al., 1990).

Abbreviations: CDC, USACenters for Disease Control and Prevention; CE, collision energy; CES, collision energy spread; DoU, degree(s) of unsaturation; ESI, electrospray ionization; EMS, eosinophilia myalgia syndrome; FDA, USA Food and Drug Administration; HPLC, high performance liquid chromatography; IDA, information-dependent acquisition; LC–MS, microcapillary HPLC-mass spectrometry; LC-UV, HPLC with UV detection; L-Trp, L-Tryptophan; NMR, nuclear magnetic resonance; MS/MS, tandem mass spectrometry; MS^n, multistage tandem mass spectrometry; PAA, 3-(phenylamino)alanine; SD, Showa Denko K.K; TOF, time-of-flight

* Corresponding author.
E-mail address: snaylor@rngen.com (S. Naylor).

http://dx.doi.org/10.1016/j.toxlet.2017.10.012
Received 4 June 2017; Received in revised form 19 August 2017; Accepted 10 October 2017
Available online 14 October 2017
0378-4274/

The SD L-Trp was produced by fermentation using a genetically engineered strain of *Bacillus amyloliquefaciens* (Belongia et al., 1992; Mayeno and Gleich, 1994). The epidemic was essentially curtailed when the FDA removed L-Trp from the retail market via a recall. Analysis of the SD L-Trp by high performance liquid chromatography (LC) and LC coupled on-line with mass spectrometry (LC–MS) revealed the presence of over sixty contaminants (Muller et al., 1991; Toyo'oka et al., 1991; Trucksess, 1993; Williamson et al., 1997). Careful and exhaustive epidemiological studies combined with sample lot analyses of this L-Trp revealed six contaminants as being case-associated with the onset of EMS. These specific contaminants were labeled as Peaks UV-5; E; 200; C; FF; and AAA; as defined by their unique LC retention times (Philen et al., 1993; Hill et al., 1993). The ensuing comprehensive analysis of SD priority case lot samples of L-Trp by Hill and coworkers revealed that of the sixty-three contaminants detected by LC-UV, only AAA was statistically significant ($p = 0.0014$) in terms of association with EMS cases. They concluded that peak AAA "should receive a high priority for isolation and identification" based on their rigorous conditional logistic regression model analysis that was also stratified by time considerations (Hill et al., 1993).

Structural characterization of five of the six case-associated contaminants has been reported previously using Nuclear Magnetic Resonance (NMR), LC–MS and tandem mass spectrometry (MS/MS). Peak UV-5 was identified as 3-(phenylamino)alanine (PAA) after isolation of the contaminant from SD L-Trp (Mayeno et al., 1992; Goda et al., 1992). Peak E was determined to be an acetaldehyde-tryptophan condensation reaction product, namely 1, 1′ ethylidenebis (tryptophan) using a combination of MS, MS/MS, nuclear magnetic resonance (NMR) and synthetic organic chemistry (Mayeno et al., 1990; Smith et al., 1991). Peak 200 has been identified as 2-(3-indolylmethyl)-tryptophan using, both NMR (Muller et al., 1991), and utilization of LC–MS and LC–MS/MS (Williamson et al., 1997). Peak C was characterized by accurate mass LC–MS, LC–MS/MS and multistage mass spectrometry (MS^n) to be 3a-hydroxy-1,2,3,3a,8,8a-hexahydropyrrolo-[2,3-b]-indole-2-carboxylic acid (Williamson et al., 1998). Peak FF was also subjected to the same analytical protocols as Peak C and identified as 2-(2-hydroxy indoline)-Trp (Williamson et al., 1998). In the case of the "high priority" contaminant peak AAA, to date and to the best of our knowledge, no complete structure determination has been reported. We report here the structural identification of the last, and highest priority case-associated contaminant peak AAA present in SD L-Trp. Peak AAA is actually, two structural aliphatic chain isomers, renamed AAA_1 and AAA_2.

2. Materials and methods

2.1. Chemicals and reagents

LC–MS grade water, methanol and acetonitrile were purchased from Millipore-Canada Ltd (Etobicoke, ON, Canada). Formic acid was obtained from either Sigma (Markham, ON, Canada) or Millipore-Canada. [Glu1]-fibrinopeptide B was purchased from Sigma. Solid phase Sep-Pak™ C-18 cartridges were obtained from Waters Corporation (Mississauga, ON, Canada). All commercially available synthetic starting materials and solvents were purchased from Sigma-Aldrich Canada (Oakville, Canada), Combi-Block Inc (San Diego, USA), Fisher Scientific Canada (Ottawa, Canada), and used as received. All reactions involving water-sensitive chemicals were carried out in oven-dried glassware with magnetic stirring under argon atmosphere.

2.2. Showa Denko L-Trp

Dr. Rossanne Philen (CDC) provided SD case implicated L-Trp. This sample lot was manufactured between January-June 1989, and had previously been demonstrated as case-implicated in EMS onset (Hill et al., 1993; Mayeno and Gleich, 1994; Philen et al., 1993). Sample storage and handling at the CDC has been described elsewhere (Hill et al., 1993; Philen et al., 1993). We received these samples on September 10th, 1996. All samples were kept in Fisher Scientific polypropylene centrifuge tubes with screw caps, under Nitrogen and further sealed with parafilm. These sample tubes were kept at −20 °C in assorted commercial freezers and out of contact with direct light except in brief instances of sample handling and preparation for analyses. In the case of sample analyses, all samples were prepared fresh on each occasion as described in Section 2.5 below.

2.3. Analytical methods for synthetic L-Trp analogs

The analytical techniques used to purify and characterize the final synthetic L-Trp analog products (**1**–**3**) were:

2.3.1. UPHPLC-UV and UPHPLC–MS

Purity was determined on a Waters UPLC H−Class (Mississauga, Canada) with UV detection, equipped with an Acquity UPLC CSH C-18 1.7 µm 2.1 × 50 mm column. MS spectra were recorded on a Waters SQD 2 detector (electrospray) instrument from Waters (Mississauga, Canada) with a linear gradient of 5–95% acetonitrile and water containing 0.1% formic acid. Final products were purified to > 95% purity (UPLC-UV) using a Waters Preparative LC (Sample Manager 2767 Fraction collector), Binary gradient module 2545, with two 515 HPLC pump and a System Fluidics Organizer, Photodiode Array Detector 2998: column X Select CSH Prep C18 5 µm OBD 19 × 250 mm column, buffer: A: 0.1% formic acid in water, B: 0.1% formic acid in acetonitrile, at a flow rate of 20 mL/min.

2.3.2. Proton nuclear magnetic resonance NMR ^1H

Proton NMR spectra were recorded with a Bruker Ascend™ 400 (Rheinstetten, Germany) operating at 400 MHz.Samples were dissolved in the indicated deuterated solvent and run at 25 °C. NMR chemical shifts are reported in ppm (parts per million) with reference to the residual peaks of the solvent. The abbreviations for peak multiplicities are described as follows: s (singlet), d (doublet), dd (doublet of doublets), t (triplet), q (quartet), qt (quintet), m (multiplet) and bs (broad singlet) for ^1H NMR.

2.4. Synthesis of L-Trp analogs

Details of the syntheses of the L-Trp analogs are described in the supplemental materials. The last steps and characterization of each synthetic compound are described here.

2.4.1. (S)-2-Amino-3-(2-((S,E)-7-methylnon-1-en-1-yl)-1H-indol-3-yl) propanoic acid (1)

Trifluoroacetic acid (TFA) (1 mL) was added directly to tert-butyl-3-((S)-2-((di-tert-butoxycarbonyl)amino)-3-methoxy-3-oxopropyl)-2-((S,E)-7-methylnon-1-en-1-yl)-1H-indole-1-carboxylate (9 mg, 0.047 mmol), stirred for 3 min, and diluted with dichloromethane. Excess TFA was co-evaporated with dichloromethane 5 times, then with diethyl ether. The resulting solid was dissolved in dioxane and treated with a NaOH (5.4 mg, 0.135 mmol) solution (1.5:1 dioxane/H_2O) for 30 min. The mixture was neutralized using 1 M HCl, and purified by preparative LC and lyophilized which yielded 2 mg of (**1**) as a white solid.

^1H NMR (400 MHz, CD_3OD) δ (ppm): 8.54, 7.63 (d, 1H), 7.30 (d, 1H), 7.10 (t, 1H), 7.00 (t, 1H), 6.65 (d, 1H), 6.27 (m, 1H), 3.91 (d, 1H), 3.9 (d, 1H) 3.13 (d, 1H), 2.27-2.22 (m, 2H) 1.63 (s, 9H) 1.49-1.44 (m, 3H) 1.35-1.29 (m, 4H) 1.16-1.09 (m, 2H) 0.86 (d, 3H) 0.84 (d, 3H).

LC–MS retention time: 1.465 min; accurate mass ESI–MS MH^+ = 343.2307, calculated for $C_{21}H_{31}N_2O_2$. Purity by LC–UV–MS, 96%

2.4.2. (S)-2-Amino-3-(2((E)-8-methylnon-1-en-1-yl)-1H-indol-3-yl) propanoic acid (2)

(S,E)-methyl 2-amino-3-(2-(8-methylnon-1-en-1-yl)-1H-indol-3-yl) propanoate (60 mg, 0.168 mmol) was dissolved in dioxane and treated with a NaOH (20 mg, 0.378 mmol) solution (1.5:1 dioxane/H_2O) for 30 min. The mixture was neutralized using 1 M HCl, purified by preparative HPLC and then lyophilized to yield 13 mg of (**2**) as a white solid.

^{1}H NMR (400 MHz, CD_3OD) δ (ppm): 7.61 (d, J = 8.0 Hz, 1H), 7.41 (d, J = 8.0 Hz, 1H), 7.24 (s, 1H), 7.12 (dd, J = 8.0, 7.4 Hz, 1H), 7.01 (dd, J = 8.0, 7.4 Hz, 1H), 5.42-5.32 (m, 2H), 4.09 (t, J = 7.2 Hz, 2H), 3.86 (dd, J = 7.1, 5.3 Hz, 1H), 3.30 (dd, J = 15.0, 5.3 Hz, 1H), 3.17 (dd, J = 15.0, 7.1 Hz, 1H), 2.06-1.97 (m, 2H), 1.97-1.89 (m, 2H), 1.77 (tt, J = 7.2, 7.2 Hz, 2H), 1.33-1.14 (m, 6H), 0.84 (t, J = 6.7 Hz, 3H).

LC–MS retention time: 1.46 min; accurate mass ESI–MS MH^+ = 343.2307, calculated for $C_{21}H_{31}N_2O_2$. Purity by LC–UV–MS, 100%.

2.4.3. (S)-2-Amino-3-(2-((E)-dec-1-en-1-yl)-1H-indol-3-yl)propanoic acid (3)

TFA (1 mL) was added directly to tert-butyl-3-((S)-2-((di-tert-butoxycarbonyl)amino)-3-methoxy-3-oxopropyl)-2-((S,E)-7-methylnon-1-en-1-yl)-1H-indole-1-carboxylate (62 mg, 0.047 mmol), stirred for 3 min, and diluted with dichloromethane. Excess TFA was co-evaporated with dichloromethane 5 times, then with diethyl ether. The resulting solid was dissolved in dioxane and treated with a NaOH (5.4 mg, 0.135 mmol) solution (1.5:1 dioxane/H_2O) for 30 min. The mixture was neutralized using 1 M HCl, purified by preparative HPLC and lyophilized to yield 20 mg of (**3**) as a white solid.

^{1}H NMR (400 MHz, CD_3OD) δ (ppm): 7.62 (d, 1H) 7.30 (d, 1H) 7.10 (t, 1H), 7.01 (t, 1H), 6.64 (d, 1H), 6.29 (m, 1H), 3.86 (dd, 1H), 3.54 (dd, 1H) 3.13 (dd, 1H), 2.30 (dd, 2H), 1,58-1.47 (m, 2H), 1.45-1.24 (m, 9H), 0.90 (t, 3H)

LC–MS retention time: 1.47 min; accurate mass ESI–MS MH^+ = 343.2307, calculated for $C_{21}H_{31}N_2O_2$. Purity by LC–UV–MS, 100%

2.5. L-Trp sample extraction

SD case-implicated L-Trp was dissolved in 50% aqueous methanol to a concentration of 20 mg/mL. Following sonication for 30 min the sample was centrifuged at 13,000 rpm using a Heraeus Biofuge (Fisher Scientific, Canada). The supernatant was diluted 10 x in water and loaded onto a methanol pre-equilibrated and water rinsed C_{18} solid phase cartridge. After an initial rinsing of the cartridge with 5% (v/v) aqueous methanol, L-Trp contaminants were eluted with 0.5 mL of methanol and vacuum dried. The sample was dissolved in 100 µL 50% (v/v) aqueous acetonitrile containing 0.2% (v/v) formic acid prior to LC–MS/MS analysis.

2.6. MS and MS/MS of L-Trp synthetic isomers

MS and MS/MS analyses of synthetic N-linked (S,Z)-2-Amino-3-(1-(dec-4-en-1-yl)-1H-indol-3-yl)propanoic acid (N-Alk-Trp), the (S,Z)-2-Amino-3-(2-(dec-4-en-1-yl)-1H-indol-3-yl)propanoic acid (**C2-Alk-Trp**) analog, as well as the C-2-linked anteiso-, iso- and linear L-Trp isomers (**1**–**3**) were performed by direct infusion on a Micromass Q-TOF-2 (Waters Corp. ON, Canada). Each synthetic L-Trp sample was diluted to 10 µM in 50% (v/v) aqueous acetonitrile containing 0.2% formic acid and infused into the ESI source via an electrospray needle (PicoTip Emitter, New Objective, MA, US) using a syringe pump (Harvard Apparatus, Holliston, MA, US) at a flow rate of 1 µL/min. The electrospray and cone voltages were set to 2100 and 45 V, respectively. Product ions were monitored consecutively using a 3-s/scan-acquisition time with the collision energy set to 25 V. Calibration was performed in MS/MS mode using fragments of [Glu1]-fibrinopeptide B, infused at a concentration of 2 µM.

2.7. Mass spectrometry of Showa Denko L-Trp

2.7.1. LC–MS and LC–MS/MS

Separations were done online using an Eksigent micro-UHPLC 200 (Sciex, California, US). Samples were injected onto a C-18 reversed phase HALO column, 100 × 0.5 mm ID, 2.7 µm particle size, 90 Å pore size (Sciex, California, US) by loop overfilling using a 5 µL injection loop. A LC gradient consisting of 0.1% (v/v) aqueous formic acid in water as Phase A, and acetonitrile with 0.1% formic acid as Phase B at a flow rate of 35 µL/min. was used with following gradient conditions: (%B/min) 15/0, 15/0.2, 30/0.5, 40/5.5, 5.6/100, 100/6.3, 15/6.4 15/7. All LC–MS and LC–MS/MS analyses were done on a Triple-TOF 5600 (Sciex, California, US) equipped with an electrospray ion source. High resolution time-of-flight (TOF)-MS survey scans (200 ms/scan, m/z 40–650) were followed by a series of 100 ms product ion scans (0.7 Da Q1 precursor window) with collision energy (CE) set to 35 V and collision energy spread (CES) of 20. The total cycle time was 750 ms. Curtain, ion source 1 and 2 gas were respectively 28, 14 and 17 L/min. In addition it is possible to combine LC–MS survey scans and up to 30 dependent MS/MS scans (accumulation time of 25 ms). This enables the selection of specific precursor ions for accurate mass LC–MS/MS determination directly from the survey scan data.

2.7.2. LC–MS^n

Separations and MS^3 analyses (fragmentation in the source followed by MS/MS of selected fragments) were done on the same LC–MS platform as described above except that a shorter column (50 mm) and following gradient was used: (%B/min) 10/0, 10/0.5, 95/2.3, 95/2.9, 10/3, 10/3.5. The ionspray voltage was set to 5.0 kV and the declustering potential was 200 V. Survey scans (m/z 50–400, 50 ms) were followed by product ion scans with a total cycle time of 875 s. The CE was 40 V with a CES of 15 V.

3. RESULTS & DISCUSSION

Previously we have reported that SD L-Trp contains over sixty different contaminants present at 0.1–0.5% of the parent compound concentration This determination was predicated on a LC–MS analysis of the SD L-Trp, in which previous analytical conditions reported by Hill were modified (Hill et al., 1993). Such changes involved the replacement of 0.1% TFA with 1% acetic acid in the LC mobile phase and the use of a narrower inner diameter LC column to ensure better interfacing with the ESI-MS interface (Williamson et al., 1997, 1998).

3.1. LC–MS detection of AAA_1 and AAA_2

We employed such analytical changes in a preliminary characterization of AAA in SD L-Trp, using a combination of accurate mass-LC–MS and LC–MS/MS (Klarskov et al., 2000). We determined that AAA had a protonated mass (MH^+) of 343.2381 Da (Da), and a LC retention time of 50.65 min (Supplemental Material Fig. S1). An accurate mass single ion monitoring LC–MS analysis of MH^+ = 343.21 − 343.25 only revealed a single ion response throughout the ion chromatogram. It should also be noted that there were other significant co-eluting ions at m/z 329 and 290 that represent fatty acid homologs of AAA_1 and AAA_2 and these compounds will be discussed in detail elsewhere (Klarskov et al., 2017).

The preliminary characterization of AAA was carried out during the period 1999–2000 and a tentative, unconfirmed structure reported (Klarskov et al., 2000). Since that time there have been further numerous analytical improvements in the LC–MS and LC–MS/MS of complex mixtures of drug metabolites, toxins and trace contaminants. The advent of reduced-flow rate capillary LC (Snyder et al., 2012), micro/nano/pico ESI-MS (Banerjee and Mazumdar, 2012), and routine accurate mass MS and MS/MS (Brenton and

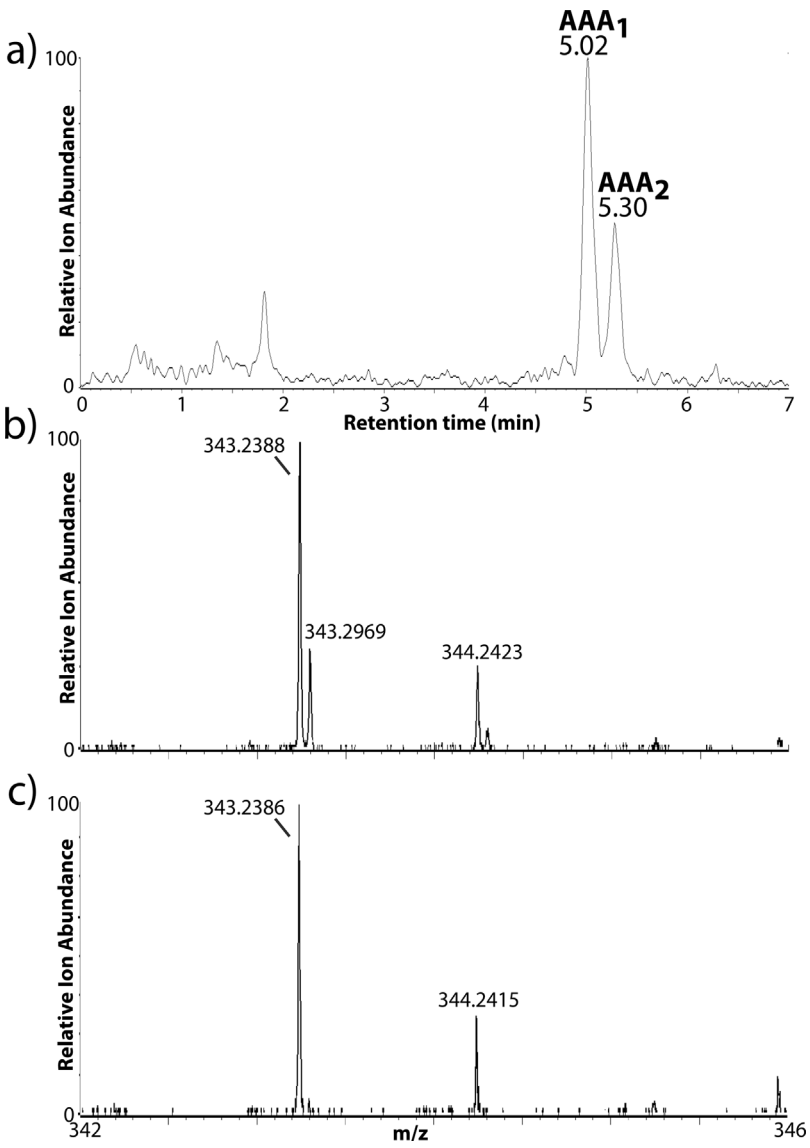

Fig. 1. Accurate mass LC–MS survey scan analysis of Showa Denko K.K. L-Trp.
a. Selected ion chromatogram for ions at *m/z* 343, retention time 0–7 min.
b. Mass spectrum for AAA_1 showing accurate mass protonated molecular ion MH^+ present in ion chromatogram peak at 5.02 min.
c. Mass spectrum mass for AAA_2 showing accurate mass protonated molecular ion MH^+ in ion chromatogram at 5.30 min.
Ions containing the C-13 isotope present in all organic compounds (1.1% of each Carbon present).

Godfrey, 2010) have resulted in a myriad of enhanced performance characteristics. They include significantly improved chromatographic resolution of complex clinical or toxicological mixtures, superior MS sensitivity and limit of detection values especially for accurate mass analysis, and facilitation of structural characterization capabilities (Pitt, 2009). We took advantages of these new improvements by employing a microcapillary LC column coupled to a microspray ion source on a Sciex 5600 accurate mass MS and MS/MS instrument in the current analyses.

In the current instance we utilized an accurate mass LC–MS survey scan in conjunction with targeted M/MS and extracted an ion analysis for MH^+ = 343. The new, enhanced analytical performance capabilities revealed an ion chromatogram containing *two* distinct ions at MH^+ = 343 Da, with LC retention times of 5.02 min and 5.30 min (see Fig. 1a). The accurate mass for protonated AAA_1 (shown in Fig. 1b) and AAA_2 (shown in Fig. 1c) was determined to be 343.2388 Da, and 343.2386 Da respectively, indicating, within the margin of error, identical masses. No other ions in the mass range *m/z* 343.21- 343.25, with the appropriate hydrophobic LC retention time properties, were detected in this LC–MS analysis (Fig. 1a). These data clearly indicate that AAA_1 and AAA_2 correspond to the chromatographically unresolved "compound AAA" detected in the original analyses and shown in Supplemental Fig. S1. In the case of AAA_1 there was a smaller co-eluting contaminant ion present at MH^+ = 343.2969 Da. The possible molecular formulae attributable to the accurate mass and the limited number of degrees of unsaturation (DoU) suggested an unknown contaminant derived from the column that co-eluted only with AAA_1.

The accurate mass determination of AAA_1 and AAA_2 suggests the same molecular formula of $C_{21}H_{30}N_2O_2$ (excluding the additional H^+ that provides the protonated positive charge) (Patiny and Borel, 2013). The molecular formula indicates that both AAA_1 and AAA_2 have eight DoU. Also, based on previous LC-UV analyses albeit of the unseparated compounds, they contain an intact indole ring with UV absorbance at 254–280 nm, accounting for six of the eight DoU (Klarskov et al., 2000). It is clear from these data that AAA_1/AAA_2 are distinctly different structures compared to the previous five case-associated contaminants Peaks UV-5 (PAA), E, 200, C, and FF. AAA_1 and AAA_2 do not contain a second L-Trp indole ring (as compared to Peak E, 200 and FF) (see Williamson et al., 1997, 1998) but appear to possess aliphatic hydrocarbon functionality, as indicated by increased LC retention time. In addition, based on the accurate mass LC–MS data AAA_1 and AAA_2 are either structural and/or stereoisomers of one another. Finally, the ratio of AAA_1: AAA_2 was determined to be ~3:1, based on the accurate mass ion chromatogram measurements of each peak (Fig. 1a).

3.2. LC–MS/MS and LC–MS^n of AAA_1 and AAA_2

We analyzed the SD L-Trp by accurate mass LC–MS/MS in order to

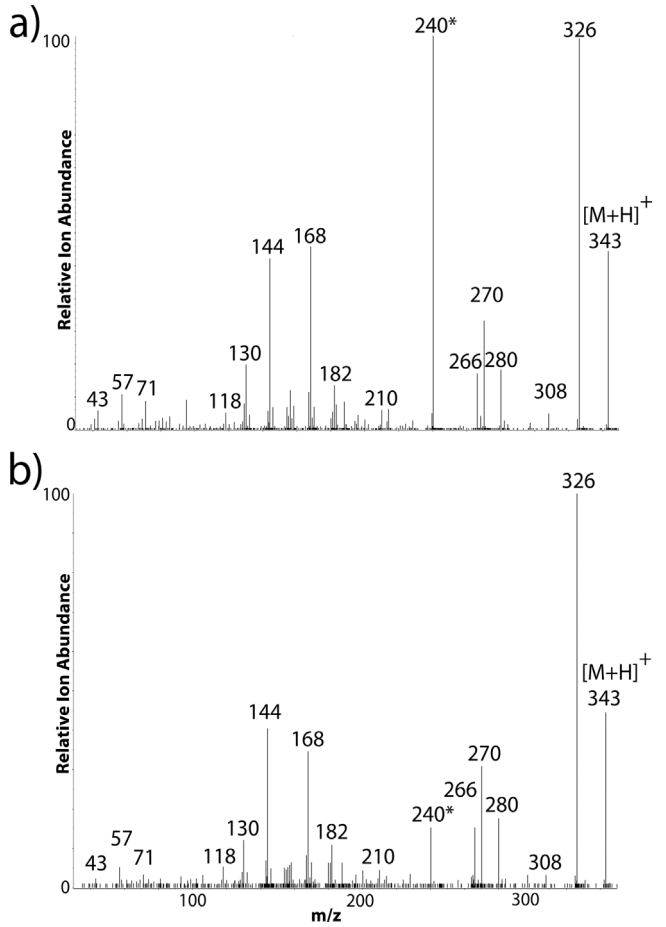

Fig. 2. Accurate mass LC–MS/MS of authentic AAA_1 and AAA_2 from SD L-Trp.
a. Product ion spectrum for AAA_1 derived from precursor ion MH^+ = 343.2388.
b. Product ion spectrum for AAA_2 derived from precursor ion MH^+ = 343.2386.
Integer product ion masses are shown for clarity, and the accurate mass values are contained in Table 1.
Note that the mass range *m/z* 40–320 is magnified threefold for clarity.
*The product ion at *m/z* 240* is a contaminant ion derived from the LC column.

elucidate the structures of AAA_1 and AAA_2. All precursor ions at MH^+ = 343 were subjected to identical ionization and collision conditions. The two resultant product ion spectra for AAA_1 (Fig. 2a), and AAA_2 (Fig. 2b) were almost identical (note that the contaminant ion MH^+ = 343.2969 present in Fig. 1b, afforded no discernible product ions under such MS/MS conditions). Since the product ion data was acquired in accurate mass MS/MS mode, it was possible to determine both the molecular ion formula and DoU for each specific product ion (Patiny and Borel, 2013). This is all summarized in Table 1 for both AAA_1 and AAA_2, in which the measured accurate mass, as well as the calculated molecular mass (predicated on molecular ion formula) is listed. The product ion spectra of AAA_1 and AAA_2 (Fig. 2a and (ed-highlight b in blue?) b respectively and Table 1) are discussed in detail below.

3.2.1. Product ion series at m/z 71, 57, and 43

Inspection of the accurate mass MS/MS spectra for AAA_1 and AAA_2 (Fig. 2a and b respectively) and Table 1, reveal a low mass product ion series at *m/z* 71, 57, and 43, each with a single DoU. Such ions are typically produced by a charge-remote fragmentation process (Demarque et al., 2016), and are indicative of an aliphatic hydrocarbon chain often derived from a fatty acid (Murphy, 2015). It has been reported that the ion at *m/z* 43 indicates the presence of an iso-branched chain, the ion at *m/z* 57 can indicate the presence of an anteiso-branched chain, and ion response at *m/z* 71 may be produced by a linear chain (Ran-Ressler et al., 2011). However, these fragmentation processes are still poorly understood, and a multitude of mechanisms for such product ion formation have been postulated (Harvey, 2005). Thus, this ion series clearly provides evidence that an aliphatic hydrocarbon chain is present but, in isolated consideration, does not provide definitive structural identity information.

3.2.2. Product ion series at m/z 144, 130 and 118

The product ions at *m/z* 144 ($C_{10}H_9N$, DoU = 7), 130 (C_9H_7N, DoU = 7) and 118 (C_8H_7N, DoU = 6) confirm the existence of an intact indole ring of L-Trp (El Aribi et al., 2004). The presence of these ions also indicates that the benzene ring (C-4 through C-7) of the indole moiety has not been substituted. For example, a MS/MS analysis of a substituted indole, e.g. 5-hyroxy-tryptophan, exhibits a product ion series at *m/z* 162, 146 and 134, reflecting the presence of a hydroxylated indole ring at C-5 (Williamson et al., 1998). All these data indicate an intact indole ring is present in AAA_1 and AAA_2, and that the benzene ring of the indole is unmodified, as highlighted in Scheme 1.

3.2.3. Product ion series at m/z 326, 308, 280 and 270

This product ion series provides structural information about the amino and carboxylic acid groups of the side-chain of L-Trp. The product ion at *m/z* 326 ($C_{21}H_{27}NO_2$, DoU = 9) is the result of a facile loss of the $-NH_3$ group from the precursor ion at MH^+ = 343 (El Aribi et al., 2004; Lioe et al., 2004). A concomitant loss of −OH affords the product ion at *m/z* 308 ($C_{21}H_{25}NO$, DoU = 10). In addition the product ions at *m/z* 280 ($C_{20}H_{25}N$, DoU = 9) and *m/z* 270 ($C_{19}H_{27}N$, DoU = 7) represent the loss of NH_3/COOH and HCN/COOH respectively, from the precursor ion (El Aribi et al., 2004; Lioe et al., 2004). This ion series and the associated fragmentation losses clearly indicate that both the L-Trp amino and carboxylic acid functional groups in AAA_1 and AAA_2 are not modified. (see Scheme 1).

3.2.4. Product ion at m/z 168, and related ions at m/z 266 and 182

The MS/MS spectra of both AAA_1 and AAA_2 contain a prominent product ion at *m/z* 168 ($C_{12}H_9N$, DoU = 9). The relative abundance of this ion indicates a facile fragmentation process that produces a stable product ion. In order to further characterize this ion we subjected it to LC–MS^n. ESI ion source fragmentation of either AAA_1 or AAA_2 resulted in the formation of *m/z* 168, which was subjected to further collision-induced dissociation in the collision cell. The resulting MS^3 spectrum for AAA_1 is shown in Fig. 3. An identical MS^n spectrum was produced by AAA_2 (data not shown). A search against MS and MS/MS databases including MassBank, the collection of tandem mass spectra of the "NIST/NIH/EPA Mass Spectral Library 2012", METLIN, and the 'Wiley Registry of Tandem Mass Spectral Data, MSforID revealed that the MS^n spectrum of AAA_1 was very similar to that of the aromatic heterocycle, carbazole (Oberacher, 2013).

It is noteworthy that the product ions at *m/z* 266 ($C_{19}H_{23}N$, DoU = 9) and 182 ($C_{13}H_{11}N$, DoU = 9) are structurally related to *m/z* 168. MS^n analyses of the *m/z* 266 and 182 ions both afford the carbazole ion at *m/z* 168 (data not shown). All these MS^n data for the product ions *m/z* 168 and 266/182 indicate that the aliphatic hydrocarbon chain is attached at the C-2 carbon of the indole ring. Furthermore these data suggest that the ninth DoU is due to a double bond at the C1′-C2′ position of the aliphatic chain. Only this regiochemistry and double bond location facilitates an energetically favoured intramolecular Diels-Alder ring formation (Demarque et al., 2016) of product ions at *m/z* 326 and 308 to afford the stable tricyclic ion at *m/z* 168, as well as the as the tricyclic product ions at *m/z* 266 and 182. This is all captured in Scheme 1.

In order to support the tentative conclusions that the aliphatic chain was attached at the C-2 indole carbon and a double bond was present at the C1′-C2′ carbons of the hydrocarbon chain, we synthesized two structural analogs of AAA_1 and AAA_2. The N-linked aliphatic chain isomer, (S,Z)-2-Amino-3-(1-(dec-4-en-1-yl)-1H-indol-3-yl)propanoic

Table 1
Accurate Mass MS/MS Product Ion Data for AAA_1, AAA_2, and Synthetic Compounds Anteiso (**1**), Iso (**2**) and Linear (**3**).

Calculated Mass	Measured Mass AAA_1	Measured Mass AAA_2	Measured Mass Anteiso	Measured Mass Iso	Measured Mass Linear	DoU[a]	Molecular Composition[b]
43.0548	43.0564	43.0580	43.0563	43.0556	43.0558	1	C3 H7
57.0704	57.0712	57.0699	57.0714	57.0720	57.0717	1	C4 H9
71.0861	71.0857	71.0865	71.0867	71.0856	71.0858	1	C5 H11
118.0657	118.0659	118.0638	118.0645	118.0652	118.0643	6	C8 H8 N
130.0657	130.0652	130.0651	130.0651	130.0656	130.0654	7	C9 H8 N
144.0813	144.0812	144.0799	144.0808	144.0809	144.0809	7	C10 H10 N
168.0813	168.0806	168.0808	168.0807	168.0813	168.0807	9	C12 H10 N
182.0970	182.0971	182.0969	182.0958	182.0972	182.0972	9	C13 H12 N
210.0919	210.0947	210.0925	210.0922	210.0910	210.0912	10	C14 H12 N O
266.1909	266.1920	266.1902	266.1914	266.1903	266.1915	9	C19 H24 N
270.2222	270.2226	270.2224	270.2221	270.2211	270.2221	7	C19 H28 N
280.2065	280.2066	280.2060	280.2057	280.2078	280.2067	9	C20 H26 N
308.2008	308.2010	308.1963	308.2012	308.2050	308.1982	10	C21 H26 N O
326.2120	326.2126	326.2125	326.2125	326.2120	326.2116	9	C21 H28 N O2
343.2386	343.2389	343.2392	343.2388	343.2396	343.2390	8	C21 H31 N2 O2
240.2333[c]	240.2327	240.2316	240.2333	240.2334	240.2308	2	C15 H30 N O

[a]DoU for the Uncharged Molecular Species.
[b]Molecular Formula for the Protonated Charged Molecular Species.
[c] The Ion at MH^+ = 240 is a Contaminant from the LC Column.

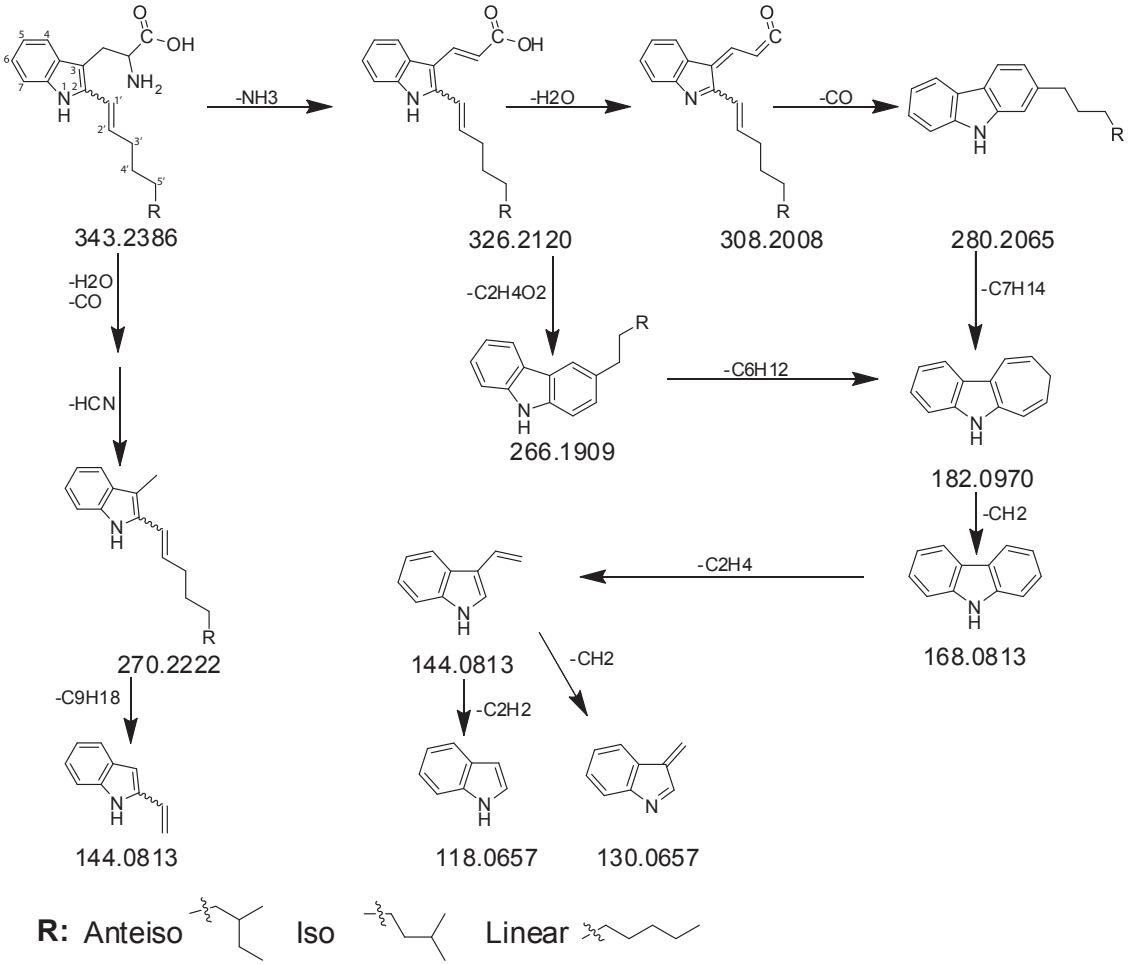

Scheme 1. Product ion spectral analysis of AAA_1 and AAA_2. Proposed product ion fragmentation pathways and structures based on MS/MS and MS^n analyses. Note that the masses shown in the Scheme represent the calculated MH^+ product ion species. The actual measured product ions for authentic AAA_1, AAA_2 and synthetic compounds (**1**–3) are shown in Table 1.

acid (**N-Alk-Trp**) was synthesized and subjected to MS/MS analysis. The product ion spectrum (shown in Supplemental Material Fig. S2) did not contain the stable carbazole tricyclic ring fragment at *m/z* 168. Instead the predominant product ion was a facile fragmentation of the heteroatom indole nitrogen and C1′ of the aliphatic chain (Demarque et al., 2016). This analysis confirms that the regiochemistry of the aliphatic chain was not at the indole nitrogen but at the C-2 of the indole ring. In addition we also synthesized a stereoisomer of AAA_1/AAA_2 in which the indole ring C-2 was linked to the aliphatic chain but with the double bond at the C4′-C5′ position of the aliphatic chain. This compound, (S,Z)-2-Amino-3-(2-(dec-4-en-1-yl)-1H-indol-3-yl)propanoic acid (**C2-Alk-Trp**) was also subjected to MS/MS analysis as shown

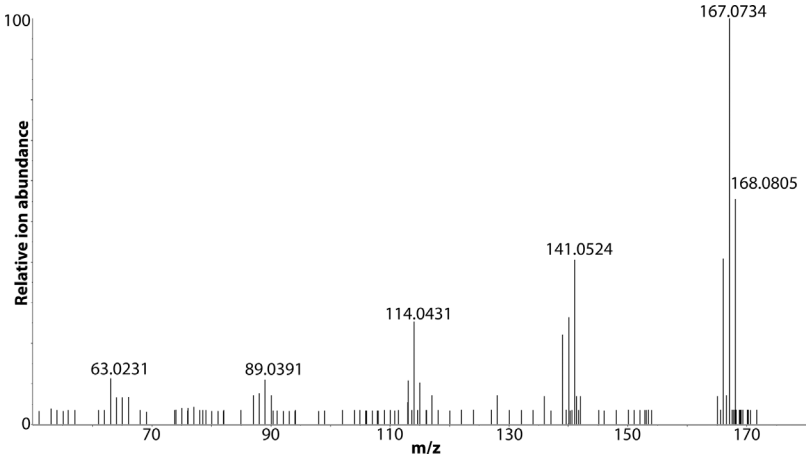

Fig. 3. LC–MS^n analysis of AAA_1. In source fragmentation of AAA_1 produced an ion at *m/z* 168. This ion was further subjected to collision induced dissociation in the collision cell to afford the MS/MS/MS spectrum shown.

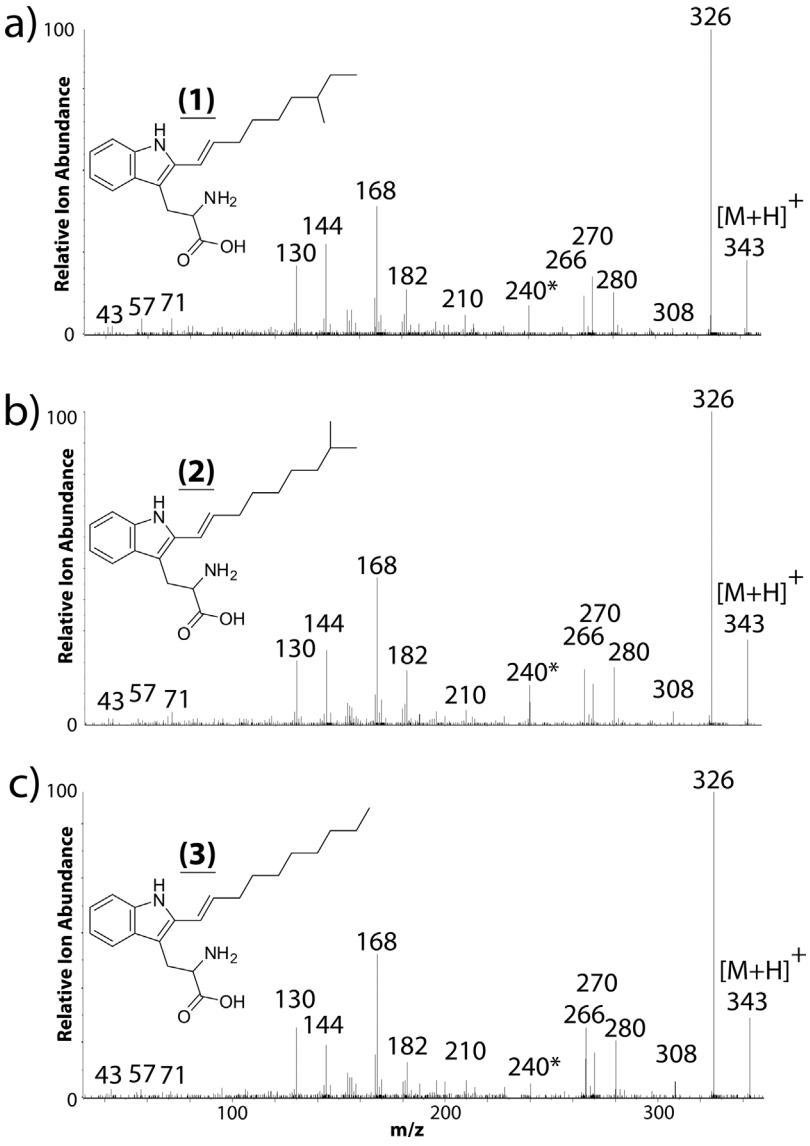

Fig. 4. Accurate mass LC–MS/MS of synthetic L-Trp isomer standards (**1–3**).
a. Anteiso isomer (**1**)
b. Iso isomer (**2**)
c. Linear isomer (**3**)
Integer product ion masses are shown for clarity, and the accurate mass values are contained in Table 1.
Note that the mass range *m/z* 40–320 is magnified threefold for clarity.
*The product ion at *m/z* 240* is a contaminant ion derived from the LC column

in Supplemental Material Fig. S3. There was no indication of the presence of the product ion at *m/z* 168, only an abundant product ion at *m/z* 202 indicative of the intact L-Trp. These data suggest that the assignment of the double bond at the C1′-C2′ position of the aliphatic chain was correct.

3.3. LC–MS and LC–MS/MS of synthetic versus SD L-Trp AAA_1 and AAA_2

We have discussed above that the aliphatic hydrocarbon chain is linked at the C-2 indole ring with a double bond at the C1′-C2′ alkyl chain. However, the stereochemistry of the C1′-C2′ double bond as well

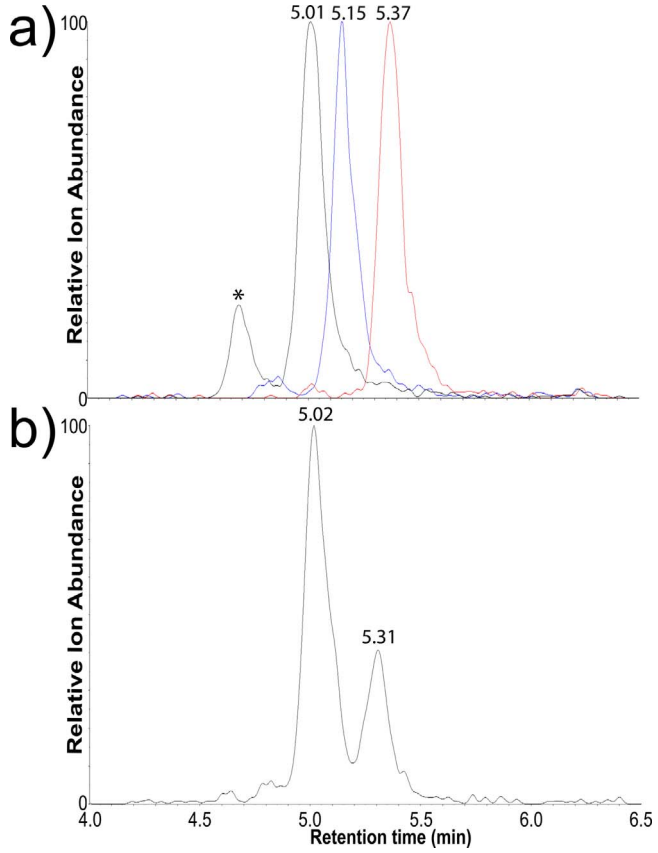

Fig. 5. Accurate mass LC–MS single ion chromatogram (MH^+ = 343).
a. Composite ion chromatogram of individual analyses of synthetic L-Trp synthetic standards
Black ion chromatogram – Synthetic Anteiso (**1**)
Blue ion chromatogram–Synthetic Iso (**2**)
Red ion chromatogram–Synthetic Linear (**3**)
b. Ion chromatogram of authentic SD L-Trp, using identical LC–MS conditions showing AAA_1 and AAA_2

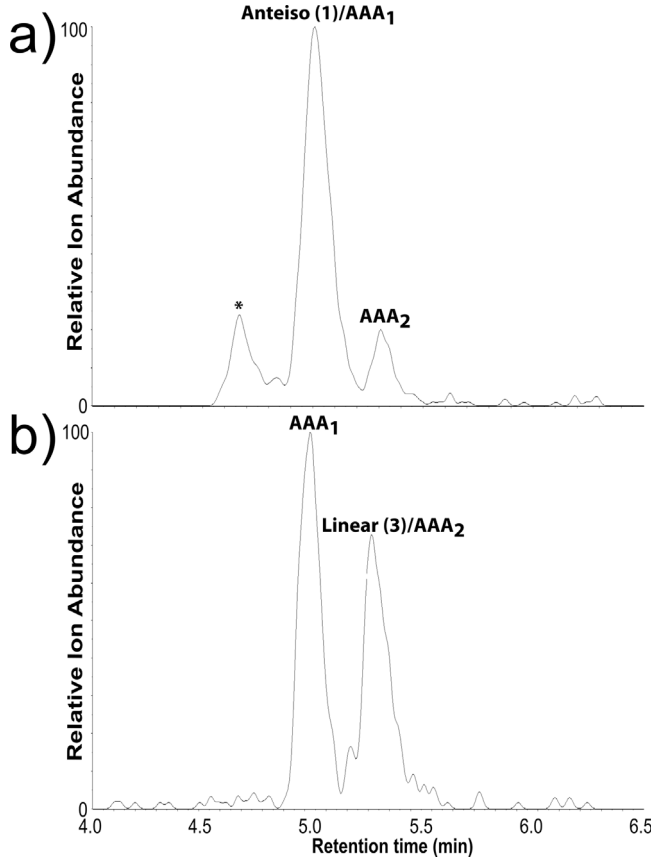

Fig. 6. Accurate mass LC–MS co-injection analyses. Ion chromatogram monitored at *m/z* 343.
a. Analysis of a mixture of an ~ equimolar mixture of synthetic standard anteiso (**1**) isomer with SD L-Trp (~1:1 of AAA_1 and anteiso (**1**)
b. Analysis of a mixture of an ~ equimolar mixture of synthetic standard linear (**3**) isomer with SD L-Trp (~1:1 of AAA_2 and linear (**3**)

as identification of the AAA_1 and AAA_2 aliphatic chain structural isomers needs to be addressed. In that regard consideration of the origin of the aliphatic chains of AAA_1 and AAA_2 is useful. It is most likely that the aliphatic chains were derived from either the free fatty acids or triglycerides present in the fermentation broth. Bacterial fatty acids are primarily found as the acyl components of phospholipids in the lipid membrane bilayer. Kaneda has stated that membrane fatty acids can be divided into two major families, namely the linear (straight chain) and branched chain fatty acids (Kaneda, 1991). In the latter case, the predominant fatty acids found in *Bacillus* species are the iso and anteiso structural isomers (see Scheme 1 for a representation of the structural differences of the two isomers). In order to control bacterial cell viability, *Bacillus* species can change membrane fluidity and permeability by altering fatty acid composition, chain length, and the ratio of branched-to-linear chain structural isomers (Diomande et al., 2015; Murínová and Dercová, 2014). These well described processes and the fatty acid constituents of *Bacillus* sp. suggest that the aliphatic chains of AAA_1 and AAA_2 were derived from C_{10} anteiso, iso or linear fatty acids.

3.3.1. LC–MS/MS

Based on consideration of all the LC–MS, LC–MS/MS and MS^n data, as well as *Bacillus* fatty acid biochemistry, we synthesized the anteiso (**1**), iso (**2**) and linear (**3**) L-Trp modified isomers (see Supplemental Materials for detailed synthetic protocols and characterization of (**1**–**3**)). The purified synthetic standards were then subjected to accurate mass MS/MS analysis under similar conditions carried out for the analyses of AAA_1 and AAA_2. The product ion spectra for anteiso (**1**), iso (**2**) and linear (**3**) are shown in Fig. 4a–c respectively. In addition the actual accurate mass MS/MS product ion data is provided in Table 1. Perusal of the MS/MS data for synthetic standards (**1**–**3**) versus authentic AAA_1 (Fig. 2a) and AAA_2 (Fig. 2b), as well as Table 1, reveals almost indistinguishable product ion spectra. We have argued above that consideration of the low mass product ion series at *m/z* 71,57, and 43 in isolation does not provide definitive evidence to distinguish anteiso, iso and linear structural isomers. However, a simple comparative pattern recognition analysis between AAA_1/AAA_2 and the synthetic standard MS/MS data tentatively suggests AAA_1 is the anteiso isomer and AAA_2 may be the linear isomer. Nevertheless we still concluded that the MS/MS and MS^n analyses alone could not provide structural data to definitively characterize AAA_1 and AAA_2.

3.3.2. LC–MS

Previously Borghi and coworkers have demonstrated that it is possible to separate Teicoplanin T- A-2 isomers using reverse phase HPLC (Borghi et al., 1991). Teicoplanin is a cyclic glycopeptide that contains seven amino acids. It can be isolated in five major isomeric forms designated T-A2-1 through T-A2-5. The isomers only differ in the structure of a single fatty acid linked via a glucosamine residue to the cyclic peptide backbone. The five fatty acid residues are 4-*n*-decenoic acid (*n*-C10:1), 8-methylnonanoic acid (iso-C10:0), *n*-decanoic acid (*n*-C10:0), 8-methyldecanoic acid (anteiso-C11:0) and 9-methyldecanoic acid (iso-C11:0). Since there is a striking structural homology to the aliphatic side chains of the synthetic standards (**1**–**3**), we developed LC conditions to separate the anteiso (**1**), iso (**2**) and linear (**3**) isomers that were compatible with ESI-MS analysis (Johnson et al., 2013).

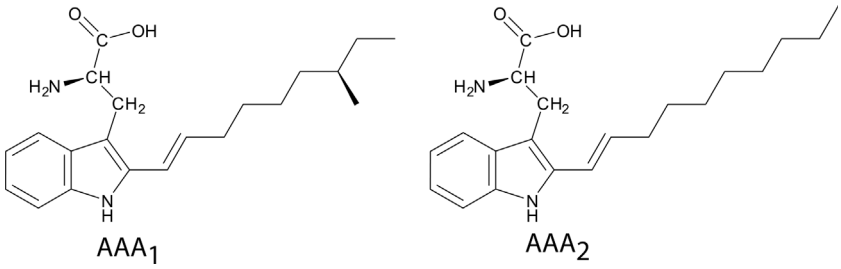

Fig. 7. Structures of AAA_1 and AAA_2.

Each of the synthetic standards (**1–3**) was injected separately at an approximate equimolar concentration, and comparative retention times were determined. All three of the individual compounds (**1–3**) could be resolved. This is shown in a composite LC–MS ion chromatogram (MH^+ = 343) with retention times of 5.01 min. (anteiso (**1**)), 5.15 min. (iso (**2**)) and 5,37 min. (linear (**3**)) for each respective isomer (Fig. 5a). There was a relatively minor contaminant present in the anteiso (**1**) compound and this can be seen in Fig. 5a, and is denoted by an asterisk. Finally it should be noted that the relative retention time elution profile of the synthetic anteiso: iso: linear isomers (**1–3**) was the same as reported for the Teicoplanin T-A2 isomers (Borghi et al., 1991).

We subsequently injected an approximate equimolar amount of authentic SD L-Trp (AAA_1: (**1**-**3**); ~1:1), under identical LC–MS conditions as for the synthetic standards. This is shown as an LC–MS ion chromatogram (MH^+ = 343) in Fig. 5b. SD- L-Trp derived AAA_1 and AAA_2 were baseline resolved with retention times of 5.02 min (AAA_1) and 5.31 min (AAA_2) respectively. Comparison of retention times (Fig. 5a and b) revealed that AAA_1 was almost identical to the anteiso standard (**1**) with a percentage change of only 0.19%. The retention time of AAA_2 most closely matched the linear compound (**3**) with a small percentage change difference of 1.3%. In the latter case it is possible that the difference in concentrations of AAA_2 compared to linear standard (**3**) led to the slight change observed in retention times.

In order to definitively confirm whether differences in retention times were due to structural components, or concentration effects, we undertook a final comparative LC–MS analysis. We took an approximate equimolar mixture (~1:1) of anteiso synthetic standard (**1**) and SD L-Trp and co-injected them together and the selected ion chromatogram (monitoring at MH^+ = 343) is shown in Fig. 6a. The synthetic anteiso standard (**1**) and authentic AAA_1 possess an identical retention time of 5.01 min, and the ratio of (AAA_1 + anteiso (**1**)) compared to AAA_2 increased from ~3:1 (see Fig. 1a) to ~6:1 (Fig. 6a) as expected. We repeated the analysis but this time co-injecting an equimolar mixture of linear synthetic standard (**3**) and SD L-Trp AAA_2. Based on the selected ion chromatogram (monitoring at MH^+ = 343), authentic AAA_2 co-eluted with linear synthetic standard (**1**). The ratio of AAA_1 to (AAA_2 + (**3**) decreased from ~3:1 (Fig. 1a) to ~3:2 as shown in Fig. 6b. These studies confirm that AAA_1 from contaminated SD L-Trp is 2-amino-3-(2-((*E*)-7-methylnon-1-en-1-yl)-1H-indol-3-yl)propanoic acid containing the anteiso derived fatty acid chain. In the case of AAA_2, it contains the linear derived fatty acid chain and confirms the identity as 2-amino-3-(2-((*E*)-dec-1-en-1-yl)-1H-indol-3-yl)propanoic acid.

The final structural consideration for AAA_1 and AAA_2 involves the configuration at the chiral centers. Showa Denko K.K. genetically engineered *Bacillus amyloliquefaciens* to only produce L-Trp (Akashiba et al., 1982). Hence the absolute configuration of the α-carbon can be assigned as (S). In addition, it has been reported that in the case of *Bacillus* sp. that produce anteiso *fatty* acids the chiral carbon containing the branched methyl group is always in the (S) configuration (Hauff et al., 2010; Christie and Han, 2010). Therefore we can further refine the structure of AAA_1 as (*S*)-2-amino-3-(2-((S,E)-7-methylnon-1-en-1-yl)-1H-indol-3-yl)propanoic acid, and AAA_2 as (*S*)-2-amino-3-(2-((*E*)-dec-1-en-1-yl)-1H-indol-3-yl)propanoic acid. These final structures are shown in Fig. 7, and presumably arise via a condensation reaction of L-Trp with the corresponding fatty acids, which possibly were incorporated, into triglyceride moieties.

The structure determination of an unknown(s) is a complicated process. Dias and colleagues in their recent paper have argued that "MS alone is not able to unambiguously identify a molecule and must rely on complementary sources of information (e.g., chromatographic retention time, or MS/MS, ….) (Dias et al., 2016). In addition they suggest, 'the currently accepted analytical standard is an isolated and authentic chemical or metabolite to which analytical data can be directly compared.' Finally the following guidelines for structure determination of metabolites and other small molecules have been met and are as follows:

1. "Confident identifications are based upon a minimum of two different pieces of confirmatory data relative to an authentic standard." We have provided three such confirmatory data sets relative to characterized synthetic standards. They include accurate mass MS, accurate mass MS/MS and MS^n, and LC–MS retention time data.
2. "Putatively annotated compounds and putatively characterized compound classes" should be compared to the metabolite or other small molecule We have discussed in detail the MS/MS spectra of authentic SD L-Trp derived AAA_1 and AAA_2 and compared and contrasted these data to that published in the literature/databases for component elements of these contaminants. Consideration of all of these elements satisfy the current criteria for the structure determination of, in this case, two case-associated small molecule contaminants found in SD L-Trp.

4. Conclusions

The thorough structure determination of the two isomers AAA_1 and AAA_2, finally completes the identification of the "six" original case-associated contaminants identified by Hill and coworkers (Hill et al., 1993; Philen et al., 1993). Simat has argued that the biotechnological manufacturing of L-Trp produces six different types of contaminants that includes i. metabolites; ii. oxidation products; iii. carbonyl condensation compounds; iv. 2-substituent −Trp derivatives; v. 1-substituent-Trp derivatives and vi. PAA and related compounds (Simat et al., 1999). AAA_1 and AAA_2 are clearly 2-substituent-Trp derivatives. However the presence of the fatty acid derived aliphatic chains in AAA_1 and AAA_2 will result in very different metabolic and distribution pathways through the body of a person consuming SD L-Trp. Whether this is of relevance in ascertaining the causal onset of EMS is still to be determined.

Conflict of interests

None

Acknowledgements

SN and GJG thank Mayo Foundation and NIH (Grant AI-31155) for funding the original work carried out at Mayo Clinic. KK acknowledges the Natural Sciences and Engineering Research Council of Canada

(NSERC-Grant RGPIN-2014-04234) and KK and EM thank the Centre de Proteomique Structurale et Fonctionnelle des Proteomes (University of Sherbrooke) for a pilot project grant. In addition we would like to thank Mr. Kenneth Johnson (Mayo Clinic) for his analytical expertise and efforts in the initial studies. Finally we would like to thank a reviewer for thoughtful and helpful suggestions.

Appendix A. Supplementary data

Supplementary data associated with this article can be found, in the online version, at https://doi.org/10.1016/j.toxlet.2017.10.012.

References

Akashiba, T., Nakayama, A. and Murata, A., (1982). Process for Producing L- Tryptophan, A Pure Culture of a Microorganism Strain used in Said Process. USA Patent 4,363, 875. December 14th, 1982.

Banerjee, S., Mazumdar, S., 2012. Electrospray ionization mass spectrometry: a technique to access information beyond the molecular weight of the analyte. Int. J. Analy. Chem., 282574. http://dx.doi.org/10.1155/2012/282574.

Belongia, E.A., Hedberg, C.W., Gleich, G.J., White, K.E., Mayeno, A.N., Loegering, D.A., Dunnette, S.L., Pirie, P.L., Macdonald, K.L., Osterholm, M., 1990. An investigation of the cause of the eosinophilia-myalgia syndrome associated with tryptophan use. N. Engl. J. Med. 323, 357–365.

Belongia, E.A., Mayeno, A.N., Osterholm, M.T., 1992. The eosinophilia myalgia syndrome and tryptophan. Annu. Rev. Nutr. 12, 235–256.

Belongia, E., 2004. Toxic Tryptophan? investigating the Eosinophilia-Myalgia syndrome in minnesota. In: Dworkin, M.S. (Ed.), Cases in Field Epidemiology: A Global Perspective. Jones & Barlett Learning, Sudbury, NA, USA, pp. 313–337 Chapter 26.

Borghi, A., Edwards, D., Zerelli, L.F., Lancini, G.C., 1991. Factors affecting the normal and branched-chain moieties of teicoplanin components produced by *Actinoplanes teichomyceticus*. J. Gen. Microbiol. 137, 587–592.

Brenton, A.G., Godfrey, A.R., 2010. Accurate mass measurement: terminology and treatment of data. J. Am. Soc. Mass Spectrom. 21, 1821–1835.

Christie, W.W., Han, X., 2010. Lipid Analysis–Isolation, Separation, Identification and Lipidomic Analysis, 4th edition. Oily Press, Bridgwater, UK.

Demarque, D.P., Crotti, A.E.M., Vessecchi, R., Lopes, J.L.C., Lopes, N.P., 2016. Fragmentation reactions using electrospray ionization mass spectrometry: an important tool for the structural elucidation and characterization of synthetic and natural products. Nat. Prod. Rep. 33, 432–455.

Dias, D.A., Jones, O.A.H., Beale, D.J., Boughton, B.A., Benheim, D., Kouremenos, K.A., et al., 2016. Current and future perspectives on the structural identification of small molecules in biological systems. Metabolites 6 (46). http://dx.doi.org/10.3390/metabo6040046.

Diomande, S.E., Nyugen-The, C., Guinebreitiere, M.-H., Brousolle, V., Brillard, J., 2015. Role of fatty acids in *Bacillus* environmental adaptation. Front. Microbiol. 6, 813. http://dx.doi.org/10.3389/fmicb.2015.00813.

Eidson, M., Philen, R.M., Sewell, C.M., Voorhees, R., Kilbourne, E.M., 1990. L-tryptophan and eosinophilia-myalgia syndrome in new Mexico. Lancet 335, 645–648.

El Aribi, H., Orlova, G., Hopkinson, A.C., Siu, K.W.M., 2004. Gas-phase fragmentation reactions of protonated aromatic amino acids: concomitant and consecutive neutral eliminations and radical cation formations. J. Phys. Chem. A 108, 3844–3853.

Goda, Y., Suzuki, J., Maitani, T., Yoshihira, K., Takeda, M., Uchiyama, M., 1992. 3-Anilino-L-Alanine structural determination of UV-5, a contaminant in EMS-associated L-Tryptophan samples. Chem. Pharm. Bull. (Tokyo) 40, 2236–2238.

Harvey, D.J., 2005. A new charge-associated mechanism to account for the production of fragment ions in the high-energy CID spectra of fatty acids. J. Am. Soc. Mass Spectrom. 16, 280–290.

Hauff, S., Rilfors, L., Hottinger, G., Vetter, W., 2010. Structure and absolute configuration of an unsaturated anteiso fatty acid from *Bacillus megaterium*. J. Chromatogr. A 1217, 1683-1687.

Hertzman, P.A., Blevins, W.L., Mayer, J.M., Greenfield, B., Ting, M., Gleich, G.J., 1990. Association of the eosinophilia-myalgia syndrome with the ingestion of tryptophan. N. Engl. J. Med. 322, 869–873.

Hertzman, P.A., Falk, H., Kilbourne, E.M., Page, S., Shulman, L.E., 1991. The eosinophilia-myalgia syndrome: the los alamos conference. J. Rheumatol. 18, 867–873.

Hertzman, P.A., Clauw, D.J., Duffy, J., Medsger Jr, T.A., Feinstein, A.R., 2001. Rigorous new approach to constructing a gold standard for validating new diagnostic criteria, as exemplified by the Eosinophilia-Myalgia syndrome. Arch. Intern. Med. 161, 2301–2306.

Hill Jr., R.H., Caudill, S.P., Philen, R.M., Bailey, S.L., Flanders, W.D., Driskell, W., Kamb, M.L., Needham, L.L., Sampson, E.J., 1993. Contaminants in L- tryptophan associated with eosinophilia- myalgia syndrome. Arch. Environ. Contam. Toxicol. 25, 134–142.

Johnson, D., Boyes, B., Orlando, R., 2013. The use of ammonium formate as a mobile-phase modifier for LC–MS/MS analysis of tryptic digests. J. Biomol. Tech. 24, 187–197.

Kaneda, T., 1991. Iso- and anteiso-fatty acids in bacteria: biosynthesis function, and taxonomic significance. Microbiol. Rev. 55, 288–302.

Kilbourne, E.M., 1992. Eosinophilia-myalgia syndrome: coming to grips with a new illness. Epidemiol. Rev. 14, 16–36.

Klarskov, K., Johnson, K.L., Gleich, G.J., Naylor, S, 2000. Structural of a contaminant in L-tryptophan associated with eosinophilia-myalgia syndrome. In: 48th American Society for Mass Spectrometry and Allied Topics Meeting. June 11–15th, 2000. Long Beach, California, USA.

Klarskov, K., Gagnon, H., Boudreault, P.-L., Normandin, C., Marsault, E., Gleich, G.J., Naylor, S., 2017. Fatty Acid Homologs of L-Tryptophan Contaminants Present in the Dietary Supplement Associated with the Onset of Eosinophilia- Myalgia Syndrome. Manuscript in preparation.

Lioe, H., O'Hair, R.A., Reid, G.E., 2004. Gas-phase reactions of protonated tryptophan. J. Am. Soc. Mass Spectrom. 15, 65–76.

Martin, R.W., Duffy, J., Engel, A.G., Lie, J.T., Bowles, C.A., Moyer, T.P., Gleich, G.J., 1990. The clinical spectrum of the eosinophilia-myalgia syndrome associated with L-tryptophan ingestion. clinical features in 20 patients and aspects of pathophysiology. Ann. Intern. Med. 113, 124–134.

Mayeno, A.N., Gleich, G.J., 1994. The eosinophilia-myalgia syndrome and tryptophan production: a cautionary tale. Trends Biotech. 12, 346–352.

Mayeno, A.N., Lin, F., Foote, C.S., Loegering, D.A., Ames, M.M., Hedberg, C.W., Gleich, G.J., 1990. Characterization of 'Peak E': a novel amino acid associated with eosinophilia-myalgia syndrome. Science 250, 1707–1708.

Mayeno, A.N., Belongia, E.A., Lin, F., Lundy, S.K., Gleich, G.J., 1992. 3- (Phenylamino) alanine, a novel aniline-derived amino acid associated with the eosinophilia-myalagia syndrome: a link to the toxic oil syndrome? Mayo Clin. Proc. 67, 1134–1139.

Muller, A., Busker, E., Gunther, K., Hoppe, B., 1991. Characterization of by-products in L-tryptophan. Bioforum 14, 350–354.

Murínová, S., Dercová, K., 2014. Response mechanisms of bacterial degraders to environmental contaminants on the level of cell walls and cytoplasmic membrane. Int. J. Microbiol. 2014http://dx.doi.org/10.1155/2014/873081. 873081 it is an Epub.

Murphy, R.C., 2015. Tandem Mass Spectrometry of Lipids: Molecular Analysis of Complex Lipids. Cambridge, UK.

Oberacher, H., 2013. Applying tandem mass spectral libraries for solving the critical assessment of small molecule identification (CASMI) LC/MS challenge 2012. Metabolites 3, 312–324.

Patiny, L., Borel, A., 2013. ChemCalc: a building block for tomorrow's chemical infrastructure. J. Chem. Int. Model 53, 1223–1228. http://www.chemcalc.org/.

Philen, R.M., Hill Jr., R.H., Flanders, W.D., Caudill, S.P., Needham, L., Sewell, L., Sampson, E.J., Falk, H., Kilbourne, E.M., 1993. Tryptophan contaminants associated with eosinophilia-myalgia syndrome. Am. J. Epidemiol. 138, 154–159.

Pitt, J.J., 2009. Principles and applications of liquid chromatography- mass spectrometry in clinical biochemistry. Clin. Biochem. Rev. 30, 19–34.

Ran-Ressler, R.R., Lawrence, P., Brenna, J.T., 2011. Structural characterization of saturated branched chain fatty acid methyl esters by collisional dissociation of molecular ions generated by electron ionization. J. Lipid Res. 53, 195–203.

Simat, T.J., Kleeberg, K.K., Muller, B., Sierts, A., 1999. Synthesis, formation and occurrence of contaminants in biotechnologically manufactured L- tryptophan. In: In: Huether, G., Kochen, W., Simat, T.J., Steinhart (Eds.), Tryptophan, Serotonin, and Melatonin: Basic Aspects and Applications, vol. 467. pp. 469–480 Adv. Expt. Med. Biol.

Slutsker, L., Hoesly, F.C., Miller, L., Williams, L.P., Watson, J.C., Fleming, D.W., 1990. Eosinophilia-myalgia syndrome associated with exposure to tryptophan from a single manufacturer. J. Am. Med. Assoc. 264, 213–217.

Smith, M.J., Mazzola, E.P., Farrel, T.J., Sphon, J.A., Page, S.W., Ashley, D., Sirimanne, S.R., Hill, R.H., Needham, L.L., 1991. 1,1'-Ethyl-idenebis(L- tryptophan), structure determination of contaminant '97'-implicated in the eosinophilia-myalgia syndrome (EMS). Tetrahedron Lett. 32, 991–994.

Snyder, L.R., Kirkland, J.J., Glajch, J.L., 2012. Practical HPLC Method Development, 2nd edition. John Wiley & Sons Inc., New York.

Swygert, L.A., Maes, E.F., Sewell, L.E., Miller, L., Falk, H., Kilbourne, E.M., 1990. Eosinophilia-myalgia syndrome: results of national surveillance. J. Am. Med. Assoc. 264, 1698–1703.

Swygert, L.A., Back, E.E., Auerbach, S.B., Sewell, L.E., Falk, H., 1993. Eosinophilia-myalgia syndrome: mortality data from the US national surveillance system. J. Rheumatol. 20, 1711–1717.

Toyo'oka, T., Yamazaki, T., Tanimoto, T., Sato, K., Sato, M., Toyoda, M., Ishibashi, M., Yoshihira, K., Uchiyama, M., 1991. Characterization of contaminants in EMS-associated L-tryptophan samples by high performance liquid chromatography. Chem. Pharm. Bull. 39, 820–822.

Trucksess, M.W., 1993. Separation and isolation of trace impurities in L- tryptophan by high performance liquid chromatography. J. Chromatogr. 630, 147–150.

UK Committee on Toxicology (COT), 2004. COT Statement on Tryptophan and the Eosinophilia-Myalgia Syndrome. Committee on the Toxicity of Chemicals in Food, Consumer Products and the Environment, United Kingdom. https://cot.food.gov.uk/sites/default/files/cot/tryptophanamend200401.pdf.

Varga, J., Jimenez, S.A., Uitto, J., 1993. L-Tryptophan and the eosinophilia- myalgia syndrome: current understanding of the etiology and pathogenesis. J. Invest. Dermatol. 100, 97S–105S.

Williamson, B.L., Benson, L.M., Tomlinson, A.J., Mayeno, A.N., Gleich, G.J., Naylor, S., 1997. On-line HPLC tandem mass spectrometry analysis of contaminants of L-tryptophan associated with the onset of the eosinophilia- myalgia syndrome. Toxicol. Lett. 92, 139–148.

Williamson, B.L., Johnson, K.L., Tomlinson, A.J., Gleich, G.J., Naylor, S., 1998. On-line HPLC tandem mass spectrometry structural characterization of case-associated contaminants of L-tryptophan implicated with the onset of eosinophilia-myalgia syndrome. Toxicol. Lett. 99, 139–150.